Volume 1 | Number 1 | Jan 2013 | Pages 1–100

Dalton Transactions

An international journal of inorganic chemistry
www.rsc.org/dalton

ROYAL SOCIETY OF CHEMISTRY

ROYAL SOCIETY OF CHEMISTRY

www.rsc.org/dalton

Graphical abstract

YC-1

?

Dalton Transactions

ARTICLE

Non-Nitric oxide Based Metallovasodilators: Synthesis, Reactivity and Biological Studies

Denise S. Sá[a,b], André F. Fernandes[b], Carlos D. S. Silva[a,b], Paula P. C. Costa[c], Manassés C. Fonteles[c], Nilberto R. F. Nascimento[c], Luiz G. F. Lopes[b] and Eduardo H. S. Sousa[b] *

There is an increasing number of compounds developed to target one or more pathways involved in vasodilation. Some studies conducted with azaindoles and indazoles derivatives showed cardiovascular activity associated to these compounds. Fast and easy structural modification of these organic molecules can be achieved using metal complexes promoting a much larger spatial change than organic strategies, potentially leading to novel drugs. Here, we have prepared a series of complexes with the formulation cis-$[RuCl(L)(bpy)_2]PF_6$, where L = 7-azaindole (ain), 5-azaindole (5-ain), 4-azaindole (4-ain), indazole (indz), benzimidazole (bzim) or quinoline (qui), which were characterized by spectroscopic and electrochemical techniques (CV, DPV). These compounds showed reasonable stability exhibiting photoreactivity only at low wavelength along with superoxide scavenger activity. Cytotoxicity assays indicated their low activity preliminarily supporting in $vivo$ application. Interestingly, vasodilation assays conducted in rat aorta exhibited great activity largely improved once compared to free ligands and even better than well-studied organic compound (BAY 41-42272), with IC_{50} reaching 55 nM. These results have validated this strategy opening new opportunities to further develop cardiovascular agents based on metallo-bicyclic rings.

1. Introduction

Cardiovascular diseases are among the highest causes of death worldwide. In many cases, the origin of these diseases are associated with disturbances in the endogenous production of cyclic guanosine-3',5'-monophosphate (cGMP), malfunctioning of cGMP-dependent kinases (PKG) and phosphodiesterase (PDE) proteins. Despite the advances in the diagnosis and treatment, cardiovascular diseases remain among the highest causes of deaths worldwide.. cGMP is an intracellular second messenger that regulates a variety of physiological processes, such as neurotransmission, relaxation of smooth muscle, regulation of blood pressure and platelet aggregation among others [1,2].

Cyclic GMP is endogenously produced from the conversion of guanosine triphosphate (GTP), which is catalyzed by soluble guanylate cyclase (sGC). This enzyme is a hemeprotein activated by nitric oxide (NO), which accelerates cGMP production up to 400-fold[3]. Once cGMP is produced it binds to PKG leading, for example, to a decrease in blood pressure. On the other hand, active PDE catalyzes the hydrolysis of cGMP disrupting this process. In cases of hypertension, the use of drugs able to stimulate the activation of sGC, PKG activation and/or inhibition of PDE5 could be essential in vasodilation[4,5]. Unfortunately, NO is not a molecule only selective to sGC, and NO donors can lead to interactions with a varied of off targets, which might cause other side effects or diseases. Therefore,

we sought to develop compounds that could act in the vasodilation process even in the absence of NO.

YC-1 (3-(5'-hidroximethil-2'-furyl)-1-benzilindazol), Figure 1, was the first synthetic organic compound to be used in the activation of sGC independent of NO[6]. This compound stimulates the activation of sGC, but the mechanism of action of YC-1 is not yet fully elucidated. Moreover, its sGC activation is not as significant as that promoted by NO, however it can cause activation in combination with carbon monoxide (CO) or subnanomolar concentration of NO[7,8]. A series of other analogous compounds were developed, e.g. BAY41-2272 (Figure 1), which has showed much higher stimulation of sGC activity, including PDE5 inhibition[4]. However, BAY41-2272 activity in inhibiting PDE5 is only significant at high concentrations, which should not be biologically relevant[9]. On the other hand, clinically used sildenafil works by inhibiting PDE5 and therefore keeps the concentration of cGMP high, as required for vasodilation. However, this drug is still dependent on the presence of normal levels of NO, whose deficiency disables or minimizes its pharmacological effect[10,11].

Given the structural limitations associated with the use of organic compounds to stimulate vasodilation, it is necessary to develop alternatives to prepare more effective drugs for this purpose[12]. It is known that transition metals compounds have the ability to alter the electronic distribution of the ligands and thus influencing their reactivity and binding to protein active site[12-19].

Additionally, a modification of organic molecules with metal complex can promote a larger structural and spatial diversity due to larger number of geometries, which has been used successfully in developing kinase inhibitors elsewhere[20,21]. Since the pharmacological activity of YC-1 and its derivatives (e.g. BAY) are based on indazoles and azaindoles (Figure 1) structures [22], we have prepared a small series of ruthenium complexes with these types of ligands and investigated their chemical and biological properties as potential vasodilators.
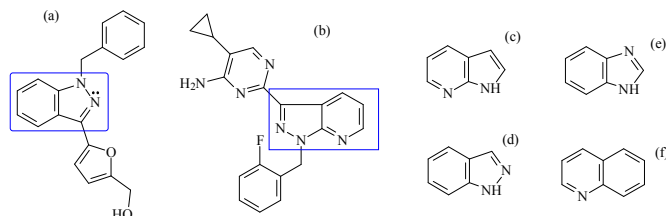
Figure 1. (a) YC-1; (b) BAY-41-2272; (c) 7-azaindole (ain) and isomers; (d) indazole(indz); (e) benzimidazole(bzim); (f) quinoline (qui).

Experimental

1.1. Materials

cis-[RuCl$_2$(bpy)$_2$] was prepared according to published procedures[23]. All other chemicals were reagent grade purchased from Sigma-Aldrich or Santa Cruz Biotechnology and used without further purification. Water used in all experiments was obtained using Direct-Q-3/UV (Millipore) system (>18 MΩ.cm).

1.2. Synthesis of *cis*-[RuCl(L)(bpy)$_2$]PF$_6$

These syntheses were based on procedures described in the literature for compounds of similar formulation[24,25]. Briefly, a 150.0 mg of *cis*-[RuCl$_2$(bpy)$_2$] **(FOR000)** (0.31 mmol) was dissolved in 20 mL of a 3:1 ethanol:water mixture and kept under argon flow and reflux for 15 minutes. After this time 0.33 mmol of the organic ligand (L) was added, previously dissolved or mixed with 5 mL of a 3:1 ethanol:water solution. This reaction mixture was kept under reflux for 2h, followed by addition of 340 mg of NH$_4$PF$_6$ (2 mmol). This solution was rotoevaporated to remove ethanol and kept in a refrigerator, then a solid was collected by filtration, washed with water and diethyl ether, dried and stored under vacuum in the absence of light. Yield was better than 80%.

1.2.1. ***cis*-[RuCl(ain)(bpy)$_2$]PF$_6$ (FOR007)**, ain = 7-azaindole. Elemental analysis, calculated (found): C: 45.55(45.73); H: 3.11(3.00); N: 11.80(11.77). ^{1}H NMR: δ(DMSO, 300 MHz) 12.21 (1H), 10.02 (1H), 8.82 (1H), 8.68 (1H), 8.62 (1H), 8.56 (1H), 8.52 (1H), 8.19 (1H), 8.09 (1H), 7.99 (1H), 7.95 (1H), 7.89 (1H), 7.82 (1H), 7.77 (1H), 7.68 (1H), 7.60 (1H), 7.58 (1H), 7.35 (1H), 7.34 (1H), 7.23 (1H),

6.87 (1H), 6.51 (1H). Electronic spectrum in acetonitrile λ(nm)/logε(M^{-1}.cm^{-1}): 243/4.44; 293/4.76; 351/4.04; 492/3.94. IR (KBr pellet, cm^{-1}): 3339; 2916; 2846; 1674; 1600; 1545; 1423 – 995; 840; 763; 729; 555; 429. Conductivity measured in acetonitrile (1 mmol L^{-1}) is 160 Scm^{2}mol^{-1} (1:1).

1.2.2. ***cis*-[RuCl(5-ain)(bpy)$_2$]PF$_6$·H$_2$O (FOR005)**, 5-ain = 5-azaindole. Elemental analysis, calculated (found): C: 45.55 (46.15); H: 3.11(3.34); N: 11.51(11.65). ^{1}H NMR: δ(DMSO, 300 MHz) 11.81 (1H), 9.96 (1H), 8.77 (1H), 8.66 – 8.50 (5H), 8.15 (1H), 8.09 (1H), 7.92 – 7.85 (5H), 7.68 (1H), 7.50 (1H), 7.38 – 7.34 (2H), 7.28 (1H), 6.57 (1H). Electronic spectrum in acetonitrile λ(nm)/logε(M^{-1}.cm^{-1}): 243/4.38; 294/4.70; 352/4.00, 513/3.90. IR (KBr pellet, cm^{-1}): 3649; 2966; 2848; 1629; 1599; 1573; 1500 – 1020; 842; 770; 727; 662; 621; 562; 421. Conductivity measured in acetonitrile (1 mmol L^{-1}) is 137 Scm^{2}mol^{-1} (1:1).

1.2.3. ***cis*-[RuCl(4-ain)(bpy)$_2$]PF$_6$ (FOR004)**, 4-ain = 4-azaindole. Elemental analysis, % calculated and (% found): C: 44.42(43.27); H: 3.11(3.11); N: 11.80(11.47). ^{1}H NMR: δ(DMSO, 300 MHz) 11.64 (1H), 9.99 (1H), 9.09 (1H), 8.81 (1H), 8.71 – 8.66 (H), 8.52 – 8.41 (2H), 8.30 (1H), 8.22 – 8.04 (H), 7.98 – 7.89 (H), 7.77 (1H), 7.69 (H), 7.58 – 7.52 (H), 7.28 – 7.24 (H), 5.84 (1H). Electronic spectrum in acetonitrile λ(nm)/logε(M^{-1}.cm^{-1}): 242/4.56; 293/4.82; 355/4.23; 497/3.99. FTIR (KBr pellet, cm^{-1}): 3432; 3092; 1623; 1603; 1563; 1503 – 973; 843; 763; 723; 653; 553; 423. Conductivity measured in acetonitrile (1 mmol L^{-1}) is 158 Scm^{2}mol^{-1} (1:1).

1.2.4. ***cis*-[RuCl(bzim)(bpy)$_2$]PF$_6$ (FOR003)**, bzim = benzimidazole. Elemental analysis, % calculated and (% found): C: 45,55(44.98); H: 3.11(3.23); N: 11.80(11.65). ^{1}H NMR: δ(DMSO, 300 MHz) 13.30 (1H), 9.25 (1H), 8.76 – 8.70 (2H), 8.57 (1H), 8.51 (1H), 8.45 (1H), 8.36 (1H), 8.13 – 8.04 (2H), 7.95 (1H), 7.87 – 7.82 (1H), 7.74 – 7.67 (2H), 7.60 – 7.54 (2H), 7.48 (1H), 7.41 (1H), 7.29 – 7.22 (2H), 7.10 – 7.05 (2H). Electronic spectrum in acetonitrile λ(nm)/logε(M^{-1}.cm^{-1}): 238/3.69; 295/3.92; 355/3.15; 502/3.11. FTIR (KBr pellet, cm^{-1}): 3660; 1620; 1600; 1567; 1500 – 1000; 846; 770; 730; 649; 599; 555; 428. Conductivity measured in acetonitrile (1 mmol L^{-1}) is 138 Scm^{2}mol^{-1} (1:1).

1.2.5. ***cis*-[RuCl(indz)(bpy)$_2$]PF$_6$·H$_2$O (FOR002)**, indz = indazole. Elemental analysis, % calculated and (% found): C: 47.42(46.28); H: 3.31(3.49); N: 11.51(11.99). ^{1}H NMR: δ(DMSO, 300 MHz) 12.94 (1H), 9.88 (1H), 8.79 – 8.35 (4H), 8.35 (1H), 8.24 – 8.11 (2H), 7.99 – 7.92 (2H), 7.86 – 7.78 (2H), 7.71 – 7.66 (2H), 7.46 – 7.30 (4H), 7.10 (1H). Electronic spectrum in acetonitrile λ(nm)/logε(M^{-1}.cm^{-1}): 242/4.34; 293/4.63; 340/3.98; 492/3.92. FTIR (KBr pellet, cm^{-1}): 3245; 3100; 2900; 1624; 1604; 1567; 1500 – 1000; 836; 770; 730; 649; 599; 552; 450. Conductivity measured in acetonitrile (1 mmol L^{-1}) is 161 Scm^{2}mol^{-1} (1:1).

1.2.6. ***cis*-[RuCl(6-COH-indz)(bpy)₂]PF₆ˑH₂O (FOR002A)**, 6-COH-indz = 1-H-indazole-6-carboxyaldehyde- Elemental analysis, % calculated and (% found): C: 44.37(44.90); H: 3.19(3.21); N: 11.09(10.99). Electronic spectra in acetonitrile λ(nm)/logℇ(M⁻¹.cm⁻¹): 237/4.65; 291/4.81; 363/4.11; 470/ 3.89. . 1H NMR: δ(DMSO, 300 MHz) 13.43 (1H), 10.07 (1H), 9.86 (1H), 8.79 (1H), 88.73 (1H), 8.68 (1H), 8.67 (1H), 8.38 (1H), 8.25 (1H), 8.17 (1H), 8.13 (1H), 7.98 (1H), 7.94 (1H), 7.84 (2H), 7.77 (1H), 7.68 (1H), 7.59 (3H), 7.39 (1H), 7.31 (1H). FTIR (KBr pellet, cm⁻¹): 3386; 2916; 2846; 1689; 1604; 1442; 1382; 1145; 840; 763; 563, 428. Conductivity measured in acetonitrile (1 mmol L⁻¹) is 145 Scm²mol⁻¹ (1:1).

1.2.7. ***cis*-[RuCl(qui)(bpy)₂]PF₆ˑCH₃Cl (FOR001)**, qui = quinoline. Elemental analysis, % calculated and (% found): C: 42.77(42.61); H: 2.87(2.92); N: 8.31(8.56). Electronic spectrum in acetonitrile λ(nm)/logℇ(M⁻¹.cm⁻¹): 228/4.54; 295/4.62; 377/3.79; 490/ 3.82. ¹H NMR: δ(DMSO, 300 MHz) 10.03 (1H), 9.87 (1H), 8.86 (1H), 8.74 (1H), 8.70 (1H), 8.38 (1H), 8.36 (1H), 8.33 (1H), 8.21 (1H), 8.19 (1H), 8.08 (1H), 8.03 (1H), 7.98 – 7.93 (3H), 7.75 – 7.69 (2H), 7.59 (1H), 7.49 (1H), 7.45 – 7.41 (2H), 7.31 – 7.24 (2H). FTIR (KBr pellet, cm⁻¹): 3050; 2823; 1608; 1593; 1473 – 1014; 827; 767; 725; 555. Conductivity measured in acetonitrile (1 mmol L⁻¹) is 144 Scm²mol⁻¹ (1:1).

1.3. Apparatus

Electronic absorption spectrum was acquired in a Cary 5000 spectrophotometer (Varian) using 1.0-cm quartz cell, where sample concentration was between 0.5×10^{-3} and 1.0×10^{-2} mol L⁻¹ for most of the experiments, unless otherwise stated. Infrared spectrum was taken on a ABB-BOMEN FTLA 2000-102 spectrophotometer, using solid samples dispersed in KBr pellets. Electrochemical experiment was done on a BAS electrochemical analyzer (Bioanalytical Systems-BAS, Epsilon model). A conventional three-electrode glass configuration cell with a glassy carbon of 0.126 cm² geometrical area, and a Pt foil was used as working and auxiliary electrodes, respectively. A 0.1 mol L⁻¹ PTBA in acetonitrile was used as electrolyte for all ruthenium complexes, at 25 ºC. Electrochemical potential value was measured versus Ag/AgCl (3.5 mol L⁻¹ KCl, BAS) as reference electrode and converted to normal hydrogen electrode (NHE) and cited accordingly throughout the text. Luminescence measurement was conducted in a 4-sided quartz cuvette with excitation and emission slits of 5nm, using a spectrofluorimeter QM-40 from Photon Technology International. NMR measurement was conducted in deuterated solvents (DMSO) using a 300 MHz. NMR Bruker. Vasodilation in aortic rings was measured by means of isometric transducers (TRI202P, Panlab, Barcelona, Spain) coupled to a data acquisition and analysis system (Powerlab, ADInstruments, Sidney, Australia).

1.4. Photochemical Studies

Continuous photolysis experiment was performed in acetonitrile, methanol and dichloromethane solutions of the complexes using a 1 cm quartz cuvette. These experiments were carried out in a photochemical reactor using lamps of 300 nm and 420 nm.

1.5. Superoxide Scavenging Assay

Superoxide was generated using hypoxanthine and xanthine oxidase enzyme system, which was measured with nitrotetrazolium blue dye (NBT) as described elsewhere[26]. This assay was conducted in 0.1 mol L⁻¹ phosphate buffer pH 7.4, containing 10 µmol L⁻¹ xanthine oxidase, 150 µmol L⁻¹ hypoxanthine, 600 µmol L⁻¹ NBT and 100 µM of metal complexes or their organic ligands (L). This reaction was kept at 25 ºC and followed for 15 min by UV-vis at 560 nm. The data was fit to a first order kinetic reaction and the maximum production of superoxide was used for comparison of scavenging efficiency. The control without metal complexes was assigned 100% and measurements taken relative to that one [26].

1.6. Vasodilation Assay

Rats were killed by overdose of sodium thiopental (150 mg. kg⁻¹). The thoracic aorta was carefully removed and cut in rings of approximately 5 mm in length. These aortic rings were mounted in a 5 mL organ bath containing Krebs- Henseleit with the following composition 120 mmol L⁻¹ NaCl, 4.7 mmol L⁻¹ KCl, 1.8 m mol L⁻¹ CaCl₂, 1.43 mmol L⁻¹ MgCl₂ , 25 mmol L⁻¹ NaHCO₃, 1.17 mmol L⁻¹ KH₂PO₄, glucose and maintained at 37ºC. After equilibration, the rings were precontracted with phenylephrine (PE, 0.2 µmol L⁻¹), and once a stable response to PE was achieved, cumulative concentration-response curves were constructed using metal-based compounds ranging from (0.1 nmol L⁻¹ up to 100 µmol L⁻¹). Tissue response was checked after these experiments to validate the tissues were still functioning properly.

1.7. Cytotoxicity assay

Cytotoxicity measurements were carried out using HCT-116, Ovcar8, HL-60 and SF295 cells obtained as a gift from National Cancer Institute, maintained in RPMI 1640 medium, supplemented with 10% FBS at 37°C in an atmosphere of 5% CO₂. Samples were evaluated using an MTT assay [27], where cells were incubated for 72 hours with 25 µg/mL of the complexes, and IC₅₀ was measured only for those compounds with at least 50% of cell death during this assay. Readings were done using a 96-well plate reader spectrophotometer at 595 nm.

2. Results and Discussion

2.1. Synthesis and characterization of complexes with formulation cis-[RuCl(L)(bpy)₂]PF₆

These complexes were prepared using a mixture of solvents ethanol/water under reflux, which enabled chloride ion substitution by aromatic ligands used in stoichiometric amounts. An earlier color change from purple to red was noticed due to the formation of aquo species [28]. Once the ligands were added a further color change was observed suggesting coordination to the ruthenium complex (Table 1). This proposal was initially supported by elemental analysis of isolated complexes, which showed values consistent with the theoretical data. Moreover, these complexes showed electronic bands in the visible range from 400 to 500 nm, which differs from the precursor with bands from 500 to 600nm (Supporting figure S1), along with bands of the ligands in the ultraviolet range. These data agreed with the better ability of the aromatic ligands to decrease LUMO energy due to backbonding effect, promoting a larger gap for electronic transitions.

Table 2. List of ligands, abbreviations and codes for complexes.

Complexes	Ligand (abbreviation)	Structure of Ligand
FOR001	quinoline (qui)	
FOR002	1H-indazole (indz)	
FOR002A	1H-indazole-6-carboxyaldehyde (6-COH-indz)	
FOR003	benzimidazole (bzim)	
FOR004	4-azaindole (4-ain)	
FOR005	5-azaindole (5-ain)	
FOR007	7-azaindole (ain)	
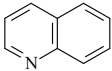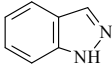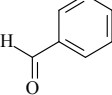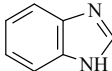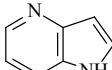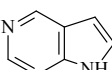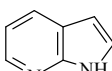
Hydrogen NMR spectra for the complexes cis-[RuCl(L)(bpy)₂]PF₆ showed signals from 13.00 to 6.00 ppm, characteristic of pyridinic derivative hydrogens, with integrations consistent with the proposed species, along with ^{13}C NMR signals found from 120 to 170 ppm (Supporting Figures S2 – S4). Moreover, all hydrogens signals between 11.00 pm and 14.00 ppm were characteristic of N-H from ligands (L), which are also observed in the free ligand. Therefore, these data indicated L was bound to the ruthenium metal complex, which causes electronic redistribution of charge particularly due to sigma bonding and backbonding effect promoted by ruthenium. Despite the fact, some complexes showed additional smaller peaks (Supporting figures S4-A/F), they were not compatible with free ligand or precursor. Besides that, those peaks were also solvent and temperature sensitive, suggesting they might come from conformational species or even linkage isomers (REF).

Molar conductivity was measured for all of these complexes at 1 mM concentration in acetonitrile. The conductivity value varied from 144 to 161 S.cm².mol⁻¹, which is indicative of cation to anion ratio of 1:1. These results are consistent with the formulation proposed for the complexes.
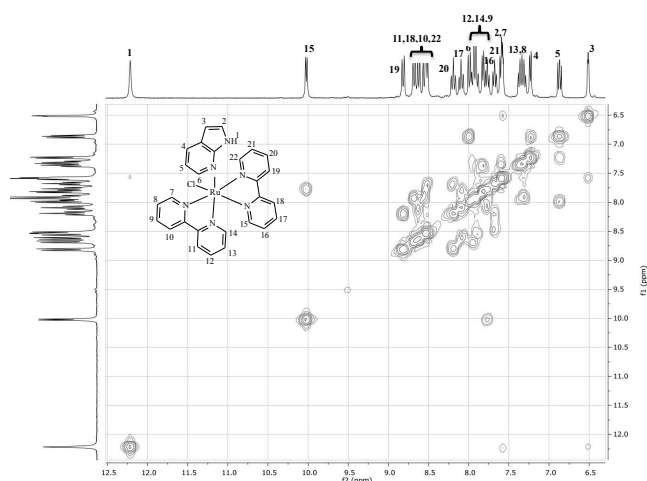
Figure 2. COSY spectrum of FOR007 (cis-[RuCl(5-ain)(bpy)₂]PF₆ in deuterated DMSO.

Figure 3 illustrates the cyclic voltammogram profile of FOR007 complex in acetonitrile (vs Ag/AgCℓ), which is similar to the other complexes synthesized (Table 1, Supporting Figure S5).
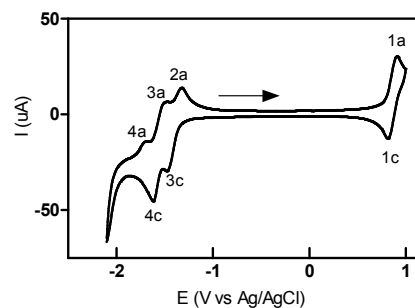
Figure 3. Cyclic voltammogram of FOR007 in acetonitrile (MeCN) /tetrabutilammonium perclorate (PTBA), 0.1 mol.L⁻¹. Rate scan: 100 mV.s⁻¹.

There is a pair of electrochemical waves (1a/1c) in the cyclic voltammograms of all complexes (Figure 3, Table 2, Supporting figure S5), which is assigned to the Ru^{III}/Ru^{II} process based on the

electrochemical behavior of similar complexes [29,30]. Comparing the oxidation potentials of these complexes to the precursor, FOR000, shown in Table 2, we observe that Ru^{II} is harder to oxidize, where the electrochemical potentials are at least +400 mV higher than the precursor. These data are consistent with the π-acceptor ability of these ligands (L) in comparison to chloride, causing stabilization of the reduced state.

The highest electrochemical potential for Ru^{III}/Ru^{II} was measured for FOR002 and FOR007, which suggests indazole and 7-azaindole are likely the strongest π-acceptor ligands among them. Similarly as reported by Cruz and colleagues[30], the waves found at negative potentials are assigned to electrochemical process involving 2,2'-bipyridine (bpy), as illustrated in scheme 1.

Table 2. Electrochemical potentials of the complexes in MeCN/PTBA (vs Ag|AgCℓ).

	1a/1c	2a	3a/3c	4a/4c
FOR000	+0.36/+0.28	-1.49	-1.73(3c)	-1.93/-1.82
FOR001	+0.87/+0.79	-1.26	-1.40(3c)	-1.70/-1.68
FOR002	+0.90/+0.82	-1.36	-1.66/-1.50	-1.75/-1.68
FOR002A	+0.94/+0.85			
FOR003	+0.76/+0.68	-1.43	-1.63/-1.43	-1.82/-1.60
FOR004	+0.78/+0.70	-1.38	-1.60/-1.43	-1.92/-1.62
FOR005	+0.78/+0.69	-1.33	-1.55/-1.51	-1.80/-1.75
FOR007	+0.91/+0.82	-1.32	-1.49/-1.48	-1.68/-1.61
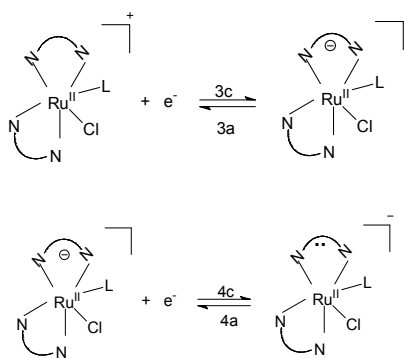
Scheme 1.

2.2. Photoreactivity

Once indazole and its isomers exhibit fluorescence, the emission spectrum of the synthesized complexes was also recorded in methanol. Figure 3 shows FOR002 emission band with maximum at 315 nm, close to free indazole (at 292 nm), but it exhibited a structured band slightly distinct. However, there is a dramatic decrease in ligand emission upon

coordination to the Ru^{II} fragment $[RuCℓ(bpy)_2]^+$, analogous behavior is observed for other complexes studied here. This type of behavior has been described before for other ligands elsewhere[31]. Interestingly, emission spectra for FOR002 showed an increased intensity at 315 nm and a shift toward a peak at 292 nm after successive measurements with excitation at 292 nm (Figure 4a). This behavior was not observed using only the free ligand (Figure 4b). These data suggested there is a photochemical reaction that takes place causing the release of the ligand (L) upon light irradiation. These spectroscopic changes were observed in methanol and acetonitrile.

Spectroscopic change of the UV-vis spectrum for FOR002 was noticed upon irradiation in acetonitrile (Supporting Figure S6-A), which was also noticed for other complexes described here. Moreover, the same final spectrum for all the complexes under study was observed, suggesting formation of the identical product after photolysis. Similar behavior was noticed upon light irradiation at 420 nm (Supporting Figure S6-B), suggesting these complexes should be protected from light.
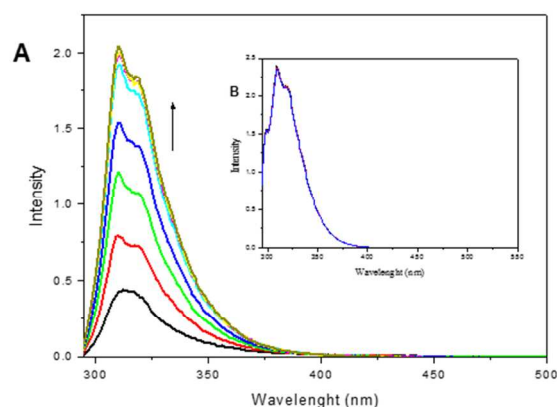
Figure 4. Emission spectrum of FOR002, 24.5 µmol L^{-1} (A), e indazole(indz) (8.2 nmol L^{-1}) (B) in MeOH, at different times of ultraviolet light irradiation. Excitation at 292 nm.

According to Cruz et al.[30] and Inglez[32] light irradiation can lead to a transient electron transfer from Ru^{II} to bipyridine promoting monodentated ligand substitution by the solvent. Once light at 300 nm and 420 nm are sufficient to form excited species of the type *cis*-$[Ru^{III}Cl(L)(bpy^-)(bpy)]^+$ it is reasonable to observe solvolysis. This is reinforced by the fact we observe identical final product after irradiation independently of the complex used (Supporting Table S1), suggesting *cis*-$[RuCl(solvent)(bpy)_2]^+$ is mainly formed. Since there is transient production of Ru^{III} complex right after irradiation, based on spectroscopic similarities, and Ru^{III}-Cl$^-$ bonding is stronger than Ru^{II}-Cl$^-$, it is reasonable to propose chloride ion is kept bound. On the other hand, aromatic ligand L can be stronger bound to Ru^{II} than Ru^{III}, once the former is a π-donor metal, so it could explain its photorelease and replacement by solvent (Supporting scheme 1). Another aspect supporting this

proposal resides on the MLCT band of *cis*-[Ru(MeCN)$_2$(bpy)$_2$]$^{2+}$ at 426 nm, which was not observed upon light irradiation

2.3. Reaction with superoxide

Cardiovascular disorders have consistently exhibited generation of radical oxygen species (ROS), including superoxide, which has been associated to tissue damage and disruption of other physiological pathways[33]. Here, we investigated the reaction of superoxide with these ruthenium-based compounds, which could eventually work preventing these harmful activities. This measurement was carried out using hypoxanthine/xanthine oxidase as superoxide generator and NBT as a detection dye. Superoxide promotes reduction of NBT to formazan, a blue dye that is used to quantify this radical as measured at 540 nm [34].

These ruthenium complexes *cis*-[RuCl(L)(bpy)$_2$]PF$_6$ were investigated to see if they were susceptible to superoxide, and their reactions were followed in buffered solution at 25 ^{o}C. Figure 5 shows FOR002 reacting with superoxide in a concentration-dependent manner, where a decrease on formazan production was observed. Similar behavior was observed for the other complexes studied here, whose values were reported as IC$_{50}$ in Table 3.
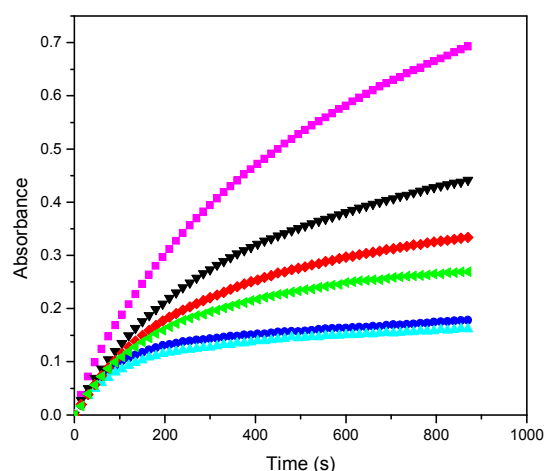
Figure 5. Reaction of ruthenium complex FOR002 with superoxide using NBT dye in phosphate buffer pH 7.4 at 25 ^{o}C, followed at 540 nm. Concentrations in µmol L^{-1}: 25 (black); 50 (red); 75 (green); 112.5 (blue); 150 (cyan) and control (magenta).

Since the formation of reduced NBT or formazan is dependent on the presence of superoxide ion [34], *cis*-[RuCl(L)(bpy)$_2$]PF$_6$ hinders the reaction of NBT with O$_2^-$. Interestingly, these complexes did not show any direct reaction with NBT neither inhibition of hypoxanthine oxidase, supporting their direct reaction with O$_2^-$.

Based on the kinetics curves showed in the Figure 5, it was determined the minimum concentration of compound required for the consumption of 50% of O$_2^-$ (IC$_{50}$) as described elsewhere [34], whose data are shown in Table 3. According to data in Table 3, FOR002 and FOR007 are the least efficient scavengers, where higher concentrations are required to deplete superoxide. On the other hand, FOR003 required only 45 µM to consume 50% of superoxide produced, almost twice more effective than others. These data are consistent with the electrochemical potential measured for Ru$^{3+/2+}$, in *cis*-[RuCl(L)(bpy)$_2$]PF$_6$ (Table 3), indicating these compounds could be indeed oxidized by superoxide produced *in vivo*.

Curiously, ruthenium complexe FOR005 displayed distinct IC$_{50}$ values toward superoxide, despite their identical electrochemical potential (Table 3). This result suggested this reaction cannot be fully explained based on their redox reaction as the driving force, but it might also involve frontier molecular orbitals as relevant for this process. Further studies are required to shed more light on this reaction.

Nevertheless, these data indicated there is a possibility of formulating complex *cis*-[RuCl(L)(bpy)$_2$]PF$_6$ working also as antioxidants in biological medium. So, these compounds could contribute to minimize oxidative stress by decreasing the concentration of O$_2^-$ in the medium. Once ROS are described as disabling sGC and also causing several diseases[35], it is interesting to remark these compounds could eventually consume one of these reactive species as well.

Table 3. Superoxide reactivity and electrochemical behavior (E$_{1/2}$) of *cis*-[RuCl(L)(bpy)$_2$]PF$_6$ versus Ag|AgCl.

Complexes	IC$_{50}$ (µmol L^{-1})	E$_{1/2}$(V)
FOR007	86	+0.87
FOR002	86	+0.86
FOR005	78	+0.74
FOR003	45	+0.72

Since, all these reactions took place in phosphate buffered solution, the stability of FOR007 was checked (*cis*-[RuCl(ain)(bpy)$_2$]$^+$) under such conditions. The appearance of a new wave at 0.41 V followed by the disappearance of a wave at 0.73V within 3 hours was noticed by differential pulse voltammetry (Supporting figure S7). Interestingly, the precursor *cis*-[RuCl$_2$(bpy)$_2$] at these conditions showed three waves at 0.30V, 0.57V (minor signal) and 0.76V, assigned to *cis*-[Ru(H$_2$O)Cl(bpy)$_2$], *cis*-[RuCl$_2$(bpy)$_2$] and *cis*-[Ru(H$_2$O)$_2$(bpy)$_2$], respectively. Additionally, once this complex was placed in 10% DMF:water a consistent increase in electrical conductivity was observed over time (Supporting figure S7). These data support a relatively fast chloride release, which was reported for other similar complexes before[36], and production of (*cis*-[Ru(H$_2$O)(ain)(bpy)$_2$]$^+$).

2.4. Vasodilation activity

Aiming to investigate the vasodilator potential for these metal-based compounds rat aortic rings pre-contracted with phenylephrine and measuring their dose-response were used. The free bicyclic ligands were also tested, but their activities were always much lower than the complexes as measured by their IC_{50} values, corresponding to the concentration to cause 50% of vasodilation. These results are shown in Figure 6 and Table 4.

Vasodilation activity was measured side-by-side with a control compound (BAY-412272), where most of the complexes showed better activity than control (Figure 6). Indeed, FOR005 was 8-fold more active than organic compound BAY-412272. Interestingly, there is a clear enhancement on vasodilatory activity upon incorporation of the metal-based fragment $[RuCl(bpy)_2]^+$. The most remarkable case was for 5-azaindole ligand, where vasodilator activity was enhanced up to 150 times upon coordination to ruthenium moiety. Preliminary data have showed FOR005 promoted a relevant increase on cGMP levels on theses tissues (Supporting figure S8). These results support this strategy as a suitable route to develop newer potent cardiovascular agents.

Table 4. Vasodilation assay for *cis*-$[RuCl(L)(bpy)_2]PF_6$ using rat aortic rings (IC_{50} values).

	Free ligand (nmol L^{-1})	Complex (nmol L^{-1})
FOR001	2300	130
FOR002	560	190
FOR002A	4300	700
FOR003	4600	n.a.
FOR005	8500	55
FOR007	4000	340

Despite the fact there is no clear correlation of structure and activity yet, it is interesting to notice the most active complex showed lower electrochemical potential than the least active. Unless we have a larger library to investigate these effects and identify hints on structure-activity we cannot assign this trend properly. Other metal complexes with distinct overall charge, backbonding effect and surrounding auxiliary ligands are going to be prepared aiming to answer these questions.
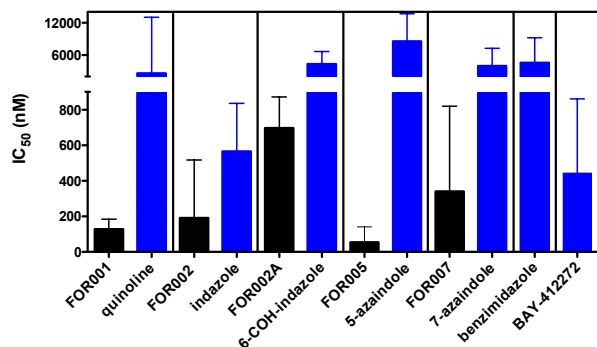
Figure 6. Measurement of vasodilation activity of *cis*-$[RuCl(L)(bpy)_2]PF_6$ (black), free ligands (blue) and BAY41-2272 (blue) using rat aortic rings.

Preliminary cytotoxicity assays were done using three cancer cell lines (human ovarian (Ovacar-8), human glioblastoma (SF-295) and human colorectal (HCT-116). However, significant blockage of cell growth was not observed (Supporting Figure S8-S10, table S2), indicating these complexes do not exhibit expressive cytoxicity. Indeed, particularly for the most active compound FOR005 with vasodilatory activity at 55 nM, even 35 µM of this compound did not show significant inhibition of cancer cell growth, suggesting a potential selectivity index for this compound above 600.

3. Conclusions

Here, we prepared and characterized a series of ruthenium-based complexes aiming to provide structural diversity to bicyclic aromatic ligands, which share similarity to organic stimulators developed for soluble guanylate cyclase. Our biological data have supported a proof-of-principle for this strategy, where azaindoles or indazoles, much simpler structures of YC-1 and BAY-412272, showed very efficient vasodilatory activity using inorganic chemistry modification, e.g. $[RuCl(bpy)_2]$. Indeed, one of these complexes, FOR005 (IC_{50} = 55 nM), was 8-fold more active than BAY-412272. Besides that, they showed apparently low cytotoxicity and promising reactivity toward superoxide, which might have further impact on the development of newer cardiovascular agents. Particularly regarding to ROS species produced during cardiovascular disorders, they have been described impairing sGC activity making nitric oxide donors ineffective. This problem has even led researches to propose co-administration of ROS scavenger agents to maximize therapy[33]. So, this work opens up new opportunities to design agents combining vasodilatory activity and potential ROS scavenger action as well in the same therapeutical agent. Unfortunately, there is no evidence these compounds promote direct activation of sGC. Indeed, preliminary studies conducted by Dr E. Martin and I. Sharina at UT Health Center at Houston did not show any significant direct activation of sGC (Supporting figure S12), despite it not being investigated upon stimulation with NO/CO or even apo-sGC. Nevertheless, we have observed a modest increase of cGMP levels measured upon FOR005 treatment, which might indicate these complexes target either NO-sGC (or oxidized sGC) and or PDE (Supporting figure S8). Mechanistic studies are going to be conducted to shed light on these biological activities.

Our lab has dedicated efforts to prepare nitric oxide donors based on ruthenium complexes[25,37-39], some of them carrying similar ruthenium moieties employed here. The activity of those complexes had been linked mainly to nitric oxide release. However, based on our data, it is possible that some activity is associated to the ruthenium product. Additionally, it is likely that a combination of the ruthenium complexes prepared here with NO could lead to even better cardiovascular agents, e.g. $[Ru(bpy)_2(5ain)(NO)]^{2+}$, which deserves further studies.

4. Notes and references

a Department of Chemistry, Federal Institute of Bahia, Salvador, Brazil 40301-150.

b Group of Bioinorganic, Department of Organic and Inorganic Chemistry, Federal University of Ceará, PO Box 6021, Fortaleza, Brazil 60440-900

c Department of Physiology and Pharmacology, Superior Institute of Biomedical Sciences, State University of Ceará, Paranjana Av, 1700, Fortaleza, Ceará , Brazil, 60740-00.

† Electronic Supplementary Information (ESI) is available: supporting figures S1 to S12, table S1-S2, scheme S1. See DOI: 10.1039/b000000x/

1. O. V. Evgenov, P. Pacher, P. M. Schmidt, G. Hasko, H. H. H. W. Schmidt and J.-P. Stasch, *Nat. Rev. Drug Discov*, 2006, 5, 755-768.
2. J. S. Bice, D. S. Burley and G. F. Baxter, *J. Cardiov. Pharmacol. Therap.*, 2014, 19, 269-282.
3. E. R. Derbyshire and M. A. Marletta, *Annu. Rev. Biochem.*, 2012, 81, 533-559.
4. J. P. Stasch and O. V. Evgenov, *Hand.b Exp. Pharmacol.*, 2013, 218, 279-313.
5. M. Zhang and D. A. Kass, *Trends Pharmacol. Sci.*, 2011, 32, 360-365.
6. F. N. Ko, C. C. Wu, S. C. Kuo, F. Y. Lee and C. M. Teng, *Blood*, 1994, 84, 4226-4233.
7. Y. S. Chun, E. J. Yeo and J. W. Park, *Cancer Lett.*, 2004, 207, 1-7.
8. M. Hoenicka, E. M. Becker, H. Apeler, T. Sirichoke, H. Schroder, R. Gerzer and J. P. Stasch, *J. Mol. Med.*, 1999, 77, 14-23.
9. F. Mullershausen, M. Russwurm, A. Friebe and D. Koesling, *Circulation*, 2004, 109, 1711-1713.
10. F. B. Priviero and R. C. Webb, *J. Cardiovasc Pharmacol*, 2010, 56, 229-233.
11. S. Gur, P. J. Kadowitz, L. Gurkan, S. Chandra, S. Y. DeWitt, A. Harbin, S. C. Sikka, K. C. Agrawal and W. J. Hellstrom, *Bju International*, 2010, 106, 78-83.
12. N. P. Barry and P. J. Sadler, *Chem. Commun.*, 2013, 49, 5106-5131.
13. E. Meggers, *Angew. Chem. Int. Ed. Engl.*, 2011, 50, 2442-2448.
14. E. H. S. Sousa, F. G. de Mesquita Vieira, J. S. Butler, L. A. Basso, D. S. Santiago, I. C. Diogenes, L. G. Lopes and P. J. Sadler, *J. Inorg. Biochem.*, 2014, 140, 236-244.
15. B. Cebrian-Losantos, E. Reisner, C. R. Kowol, A. Roller, S. Shova, V. B. Arion and B. K. Keppler, *Inorg. Chem.*, 2008, 47, 6513-6523.
16. E. H. S. Sousa, D. L. Pontes, I. C. Diogenes, L. G. Lopes, J. S. Oliveira, L. A. Basso, D. S. Santos and I. S. Moreira, *J. Inorg. Biochem.*, 2005, 99, 368-375.
17. M. Dorr and E. Meggers, *Curr. Opin. Chem. Biol.*, 2014, 19, 76-81.
18. J. X. Ong, C. W. Yap and W. H. Ang, *Inorg. Chem.*, 2012, 51, 12483-12492.
19. A. J. Salmon, M. L. Williams, A. Innocenti, D. Vullo, C. T. Supuran and S. A. Poulsen, *Bioorg. & Med. Chem. Lett.*, 2007, 17, 5032-5035.
20. L. Feng, Y. Geisselbrecht, S. Blanck, A. Wilbuer, G. E. Atilla-Gokcumen, P. Filippakopoulos, K. Kraling, M. A. Celik, K. Harms, J. Maksimoska, R. Marmorstein, G. Frenking, S. Knapp, L. O. Essen and E. Meggers, *J. Am. Chem. Soc.*, 2011, 133, 5976-5986.
21. J. Maksimoska, L. Feng, K. Harms, C. Yi, J. Kissil, R. Marmorstein and E. Meggers, *J. Am. Chem. Soc.*, 2008, 130, 15764-15765.
22. O. V. Evgenov, P. Pacher, P. M. Schmidt, G. Hasko, H. H. Schmidt and J. P. Stasch, *Nat. Rev. Drug. Discov.*, 2006, 5, 755-768.
23. B. P. Sullivan, D. J. Salmon and T. J. Meyer, *Inorg. Chem.*, 1978, 17, 3334-3341.
24. M. G. Sauaia, F. D. S. Oliveira, R. G. de Lima, A. D. L. Cacciari, E. Tfouni and R. S. da Silva, *Inorg. Chem. Comm.*, 2005, 8, 347-349.
25. F. O. N. Silva, S. X. B. Araujo, A. K. M. Holanda, E. Meyer, F. A. M. Sales, H. C. N. Diogenes, I. M. M. Carvalho, I. S. Moreira and L. G. F. Lopes, *Eur. J. Inorg. Chem.*, 2006, 2020-2026.
26. M. Younes and U. Weser, *FEBS letters*, 1976, 61, 209-212.
27. T. Mosmann, *J. Immunol. Methods*, 1983, 65, 55-63.
28. J. B. Godwin and T. J. Meyer, *Inorg. Chem.*, 1971, 10, 471-474.
29. R. W. Callahan, G. M. Brown and T. J. Meyer, *Inorg. Chem.*, 1975, 14, 1443-1453.
30. A. J. Cruz, R. Kirgan, K. Siam, P. Heiland and D. P. Rillema, *Inorg. Chim. Acta*, 2010, 363, 2496-2505.
31. G. J. Wilson, A. Launikonis, W. H. F. Sasse and A. W. H. Mau, *J. Phys. Chem. A*, 1997, 101, 4860-4866.
32. S. D. Inglez, F. C. A. Lima, M. R. Camilo, J. F. S. Daniel, E. D. A. Santos, B. S. Lima-Neto and R. M. Carlos, *J. Braz. Chem. Soc.*, 2010, 21, 157-168.
33. T. Munzel, T. Gori, R. M. Bruno and S. Taddei, *Eur. Heart J.*, 2010, 31, 2741-2748.
34. M. Younes and U. Weser, *FEBS Letters*, 1976, 61, 209-212.
35. F. B. Priviero, S. M. Zemse, C. E. Teixeira and R. C. Webb, *Am. J. Hypertens.*, 2009, 22, 493-499.
36. N. R. Davies and T. L. Mullins, *Aust. J. Chem.*, 1967, 20, 657-668.
37. A. K. M. Holanda, D. L. Pontes, I. C. N. Diógenes, I. S. Moreira and L. G. F. Lopes, *Trans. Metal Chem.*, 2004, 29, 430.
38. F. O. N. da Silva, E. C. C. Gomes, T. D. Francisco, A. K. M. Holanda, I. C. N. Diogenes, E. H. S. de Sousa, L. G. F. Lopes and E. Longhinotti, *Polyhedron*, 2010, 29, 3349-3354.
39. L. G. F. Lopes, E. H. S. Sousa, J. C. V. Miranda, C. P. Oliveira, I. M. M. Carvalho, A. A. Batista, J. Ellena, E. E. Castellano, O. R. Nascimento and I. S. Moreira, *J. Chem. Soc.-Dalton Trans.*, 2002, 1903-1906.